Am J Physiol Cell Physiol 288: C72–C80, 2005.
First published September 22, 2004; doi:10.1152/ajpcell.00056.2004.

Cell stiffness and receptors: evidence for cytoskeletal subnetworks

Hayden Huang,[1] Jeremy Sylvan,[1] Maxine Jonas,[2] Rita Barresi,[3] Peter T. C. So,[2] Kevin P. Campbell,[3] and Richard T. Lee[1]

[1]*Cardiovascular Division, Department of Medicine, Brigham and Women's Hospital, Harvard Medical School, Cambridge;* [2]*Biological Engineering Division, Massachusetts Institute of Technology, Cambridge, Massachusetts; and* [3]*Department of Physiology and Biophysics and Department of Neurology, Howard Hughes Medical Institute, Roy J. and Lucille A. Carver College of Medicine, University of Iowa, Iowa City, Iowa*

Submitted 27 January 2004; accepted in final form 16 September 2004

Huang, Hayden, Jeremy Sylvan, Maxine Jonas, Rita Barresi, Peter T. C. So, Kevin P. Campbell, and Richard T. Lee. Cell stiffness and receptors: evidence for cytoskeletal subnetworks. *Am J Physiol Cell Physiol* 288: C72–C80, 2005. First published September 22, 2004; doi:10.1152/ajpcell.00056.2004.—Viscoelastic models of cells often treat cells as homogeneous objects. However, studies have demonstrated that cellular properties are local and can change dramatically on the basis of the location probed. Because membrane receptors are linked in various ways to the intracellular space, with some receptors linking to the cytoskeleton and others diffusing freely without apparent linkages, the cellular physical response to mechanical stresses is expected to depend on the receptor engaged. In this study, we tested the hypothesis that cellular mechanical stiffness as measured via cytoskeletally linked receptors is greater than stiffness measured via receptors that are not cytoskeletally linked. We used a magnetic micromanipulator to apply linear stresses to magnetic beads attached to living cells via selected receptors. One of the receptor classes probed, the dystroglycan receptors, is linked to the cytoskeleton, while the other, the transferrin receptors, is not. Fibronectin-coated beads were used to test cellular mechanical properties of the cytoskeleton without membrane dependence by allowing the beads to endocytose. For epithelial cells, transferrin-dependent stiffness and endocytosed bead-dependent stiffness were similar, while dystroglycan-dependent stiffness was significantly lower. For smooth muscle cells, dystroglycan-dependent stiffness was similar to the endocytosed bead-dependent stiffness, while the transferrin-dependent stiffness was lower. The conclusion of this study is that the measured cellular stiffness is critically influenced by specific receptor linkage and by cell type and raises the intriguing possibility of the existence of separate cytoskeletal networks with distinct mechanical properties that link different classes of receptors.

magnetic micromanipulator; dystroglycan; transferrin

THE MECHANISM BY WHICH CELLS sense and respond to mechanical forces is relevant to many pathological conditions, such as atherosclerosis and myopathies. While there is no consensus regarding the specific response mechanism, it is thought that the cytoskeleton plays an important role in sensing the cell's physical environment (9, 32, 33). To study the cellular response to mechanical stresses, different methods have been used, including membrane strain studies (6, 8, 11, 15, 28, 37, 39, 50) and cone viscometer experiments (49). More recently, new techniques have allowed greater control of the applied forces and the targeting of specific membrane receptors (1, 5, 12, 21, 23, 35, 42, 47, 48). Magnetic micromanipulation applies stresses via magnetic beads and is capable of generating either linear (1, 4, 42) or twisting stress (10, 43, 44, 52, 53). Mechanical stresses applied to different receptors using magnetic micromanipulation result in molecular signaling that is strongly present only when the receptor stressed is cytoskeletally linked (2, 41–43). These results support the notion that cytoskeletally linked receptors serve as a link between the external mechanical environment and the internal signaling domains of the cell. Tensegrity-based models carry this notion further, leading to the hypothesis that stressing cytoskeletally linked receptors results in a significant geometric change in the cell cytoskeleton, in turn leading to the activation of specific signaling pathways (26, 31, 32, 45, 54). If hypotheses such as this one are true, then the molecular responses of the cell is likely to be different, depending on whether the receptor stressed was linked to the signaling pathway (the cytoskeleton). In the present study, we have examined whether the mechanical responses of cells are receptor dependent. To address this issue, mechanical properties of cells were measured by stressing two receptors, transferrins and dystroglycan, as well as beads that were endocytosed. We tested the hypothesis that cells probed via the cytoskeletally linked receptor would exhibit mechanical properties different from those of the non-cytoskeletally linked receptor. Endocytosed beads would represent a more global cytoskeletal resistance without any receptor specificity.

Integrins are transmembrane heterodimers that consist of an α- and a β-subunit. Fibronectin adheres predominantly to a subset of β_1 integrins that are linked to the cytoskeleton via cytoskeleton-associated proteins such as vinculin and talin. Most work on the cellular response to mechanical stimuli has targeted these receptors. Transferrin receptors mediate the transportation of iron-bound transferrin into the cell; these receptors have been shown to diffuse freely when observed within a short time frame and are thought to demonstrate the mosaic compartmentalization model of the cell membrane (22).

Dystroglycan is a laminin-binding receptor that links to the cellular cytoskeleton via dystrophin/utrophin molecules (27, 30). The dystroglycan receptor is composed of two subunits, α- and β-dystroglycan, with α-dystroglycan located outside the cell and the transmembrane β-subunit linking indirectly to the cytoskeleton. In striated muscle, dystroglycan is a part of the dystrophin-glycoprotein complex (DGC), and defects of the DGC can cause muscular dystrophy and may lead to heart failure (13, 14, 18, 29, 38, 40). While dystroglycan is considered an adhesion receptor because of its interaction with the extracellular matrix and cytoskeleton, the role that dystrogly-

Address for reprint requests and other correspondence: H. Huang, 65 Landsdowne St., Rm. 283, Cambridge, MA 02139.

The costs of publication of this article were defrayed in part by the payment of page charges. The article must therefore be hereby marked "*advertisement*" in accordance with 18 U.S.C. Section 1734 solely to indicate this fact.

 0363-6143/05 $8.00 Copyright © 2005 the American Physiological Society

can plays in cell signaling is unclear. Because little is known about dystroglycan interactions with the physical environment and because defects in the DGC affect mechanically active tissues, determining the mechanical properties of the cell via this receptor is an important first step toward characterizing its potential role in mechanotransduction.

Magnetic twisting has revealed that cells stressed via integrins appear stiffer by a factor of 3–10 compared with stressing via the nonintegrin receptors (53). However, magnetic twisting results are affected by heterogeneity of bead attachments and are harder to visualize as a physical model (7, 20). Beads coated with adhesion molecules against integrins also tend to be endocytosed if left on the cells for extended times. As a result, a need exists to broaden testing by using a different technique and to test other receptors linked to the cytoskeleton that do not follow the integrin-vinculin-actin motif. In addition, there has been little formal characterization of potential differences in cell stiffness across different cell types. Considerations of this variance in cell stiffness are important because different types of cells may have mechanical properties that reflect their physiological functions.

METHODS

Bead protocol. Unless otherwise noted, chemicals were obtained from Sigma (St. Louis, MO). Fibronectin was acquired from Invitrogen (Carlsbad, CA). Antibodies against the transferrin receptor were purified using a protein A affinity chromatography column obtained from Bio-Rad (Hercules, CA). Dynabeads M-450 tosylactivated paramagnetic beads (Dynal, Oslo, Norway), 4.5 μm in diameter, were coated with adhesion proteins and antibodies. Source beads (0.5 ml at 4×10^8 beads/ml) were washed in either 0.1 M phosphate buffer, pH 7.4 (for antibody coating), or 0.1 M borate buffer, pH 9.5 (for fibronectin coating), and were resuspended in the same buffer. Adhesion protein or antibody (5 μg/10^7 beads) was then added, corresponding to a total of 100 μg of protein/0.5 ml of bead coating. The remainder of the coating protocol followed the manufacturer's instructions and included 0.02% sodium azide supplementation for bead storage at 4°C.

Cell culture. Human embryonic kidney (HEK)-293 cells and human aortic smooth muscle cells were grown in standard 150-cm^2 culture flasks (Corning/VWR International, West Chester, PA) in DMEM (Biowhittaker/Cambrex, Walkersville, MD) supplemented with penicillin/streptomycin (100 U of penicillin/ml medium; 100 μg of streptomycin/ml medium; GIBCO-BRL, Carlsbad, CA) and 10% fetal bovine serum (HyClone, Logan, UT). Cells were passaged into 35-mm cell culture dishes for adherent cells (Corning/VWR International) and cultured for 1–3 days until confluent. Human aortic smooth muscle cells were used only until *passage 7*.

One hour before the magnetic trap experiment, 0.5–2 μl (concentration 4×10^8 beads/ml) of magnetic beads were applied to confluent 35-mm cell culture dishes. Immediately before the experiment, nonadherent beads were washed off with two washes using culture medium. The 35-mm cell culture dish was then placed into a temperature-controlled microscope chamber for force application. In other experiments, 1 μM cytochalasin D was added to the cell culture dish for 15 min before experimentation to test the changes in cell properties after the disruption of the actin cytoskeleton. For each cell type, a different dish was used for each bead coating.

Transmission electron microscopy revealed that while the transferrin- and dystroglycan-coated beads remained outside the cells after incubation, all of the fibronectin-coated beads were internalized by the end of a 1-h incubation [data not shown; other examples of scanning and transmission electron microscopy can be found in the literature (10, 20, 42)]. Thus the results of fibronectin-coated bead analysis reflect the internal cytoskeleton in a membrane-independent fashion.

Magnetic trap and microscope. The magnetic trap was custom made from CMI rod (CMI Specialty Materials, Cheshire, CT) and manually wrapped with 350 turns of 18-gauge copper wire (Newark Electronics, Chicago, IL). For experiments, a magnetic trap was placed in a micromanipulator beside an inverted Olympus IX-70 fluorescent microscope (Olympus, Melville, NY) with a charge-coupled device (CCD) camera (Roper Scientific, Trenton, NJ) (Fig. 1*A*).

Calibration of the magnetic traps was performed using magnetic beads suspended in polysiloxane. The bead displacement was captured as a movie using the CCD camera while constant current was applied to the magnetic trap wires. The movie was then postprocessed, and the velocity of the bead was extracted using a custom MatLab program (Mathworks, Natick, MA). The velocity was then converted to force as a function of distance using the Stokes formula (36). This procedure was repeated for three beads, and the best fitting force function was used (Fig. 1*B*).

The experiments were performed using a similar protocol. After the cells were loaded with beads and placed onto the temperature-controlled stage maintained at 37°C, 8-s movies were captured using the CCD camera (see movie frame shown in Fig. 1*C*). The magnetic trap was positioned at a fixed angle to the dish to generate a consistent, horizontal pulling force on the beads during current flow. The magnetic trap was off during the first 2 s, then on for the next 3 s, and then off for the final 3 s. While on, the magnetic trap was set for current ranging from 0.3 to 1 A. The movie was then analyzed for magnetic bead displacements using a custom MatLab program to fit to a cell model. The total experimental time frame per cell was kept short so that active remodeling of the cell could be neglected. At least 30 beads per bead coating were used, with beads at least 1 mm away from the previously used beads in the same dish selected to minimize remodeling effects. Cytochalasin D-treated cells were used in separate dishes from the untreated cells. The total duration of the stressing experiments was ~30 min/dish.

Cell model. Magnetic bead displacements were analyzed using the dashpot-Kelvin body model presented by Bausch et al. (3, 4). Analyses of magnetic bead motion are useful because the results characterize the local cell stiffness and time-dependent deformation of the mechanical responses of the cells. Magnetic beads of three coatings were used for comparison: fibronectin, anti-transferrin antibody (W632), and anti-dystroglycan antibody (VIA_4). Bead displacement curves for a given experiment were normalized by force and then fit for η_0, η_1, k_0, and k_1 to the dashpot-Kelvin body model using MatLab's nonlinear fitting function to the loading portion of the response curve (Fig. 2*A*). The local cell stiffness, $k_0 + k_1$, the relaxation time, $\eta_1(k_0 + k_1)/k_0k_1$, and the viscous friction coefficient, η_0, were derived from the parameters, and the 10–90% range for each parameter was compared for statistical differences among the different receptor types. Extreme outliers were discarded before the 10–90% range determination to eliminate data from poorly bound beads or other experimental anomalies. The 10–90% range was determined by sorting the parameters according to their amplitude and then excluding the highest and lowest 10%. This procedure was performed to reduce the contribution of outliers, especially outliers above median that had large variances. Magnetic bead displacements were analyzed for both epithelial and smooth muscle cells.

Receptor-tracking experiments. To test the linkage of the receptors to the cytoskeleton, small gold particles were attached to the different receptors and tracked over time to measure the amount of receptor displacement. This concept is based on the study by Fujiwara et al. (22), who showed that transferrin receptors exhibit compartmentalized random walks. It was expected that the transferrin receptors on the epithelial cells would also exhibit similar behavior, whereas the β_1 integrin and dystroglycan receptors are not free to diffuse, because of their linkage to the cytoskeleton. While fibronectin engages many different integrins, its primary attachment is via the β_1 integrin

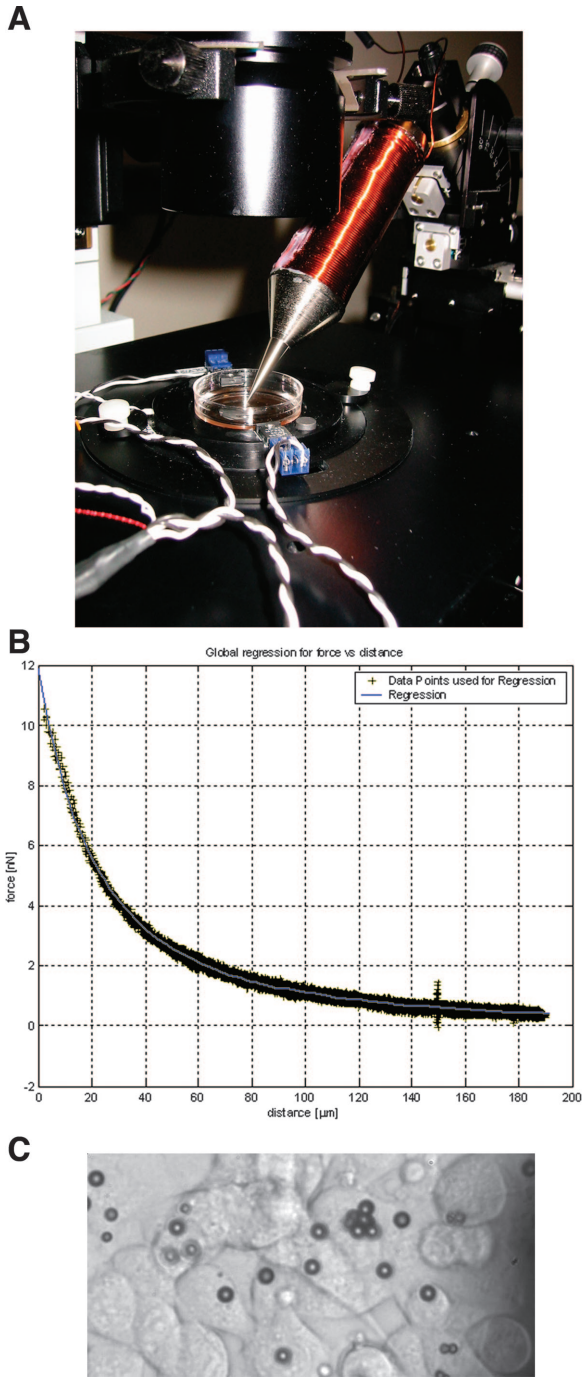

Fig. 1. *A*: the magnetic trap used for applying a controlled force to cells via magnetic beads is shown in a setup on the microscope stage, which is placed into a micromanipulator with stage heater. *B*: typical calibration curve showing the drop-off in force with distance away from the trap tip. The calibration was obtained by suspending magnetic beads in a viscous solution, tracking the velocity, and applying the Stokes formula. *C*: a sample image of epithelial cells loaded with magnetic beads. The shadow along the *right* side of the image is the tip of the magnetic trap. The magnetic beads shown are 4.5 μm in diameter.

subunit. Thus the β_1 antibody was used instead of fibronectin because fibronectin causes aggregation when coating small particles.

Streptavidin-coated gold nanoparticles (Research Diagnostics, Flanders, NJ), 30–40 nm in size, were linked to antibodies against the dystroglycan receptor, the transferrin receptor, and the β_1 integrin subunit (Research Diagnostics). The antibodies were biotinylated using the ProtOn kit (Vector Laboratories, Burlingame, CA) according to the manufacturer's protocol. One microgram of the biotinylated antibody was incubated with 10 μl of the nanoparticles (stock solution 20 μg/ml) for 5 min at room temperature and stored at 4°C. Coated gold nanoparticles were added to dishes containing HEK-293 cells and incubated for 1 h at 37°C. The motion of the nanoparticles was then tracked by acquiring images of the same particle every minute for 4 min and using a custom MatLab program to determine the particle locations in each image. Particle displacements then were calculated for each minute of the 4-min interval, from *time 0* to 1 min, then from *time 1* to 2 min, and so forth, and afterward the four displacements were averaged. The time of 1 min between frames was selected to help ensure that the nanoparticle had sufficient time to move out of at least a single compartment, if applicable. The receptor-tracking experiments were performed for the epithelial cells, but not for smooth muscle cells, because the latter tend to rapidly engulf small particles.

Statistics. The Kruskal-Wallis nonparametric test and the Dunn's posttest were used to compare medians for the three-magnetic-bead model physical parameters. The Mann-Whitney nonparametric test was used to test for significant differences between the untreated cell and the cytochalasin D-treated cell for the same receptor type. The median displacements of the gold nanoparticles were compared using the Kruskal-Wallis nonparametric test and the Dunn's posttest. GraphPad Instat software (San Diego, CA) was used for the nonparametric analyses, and $P < 0.05$ was considered statistically significant.

RESULTS

The magnetic trap calibration showed that the force exerted on the magnetic beads was in the range of 0.3–3 nN. The currents used to generate this level of force ranged from 0.3 to

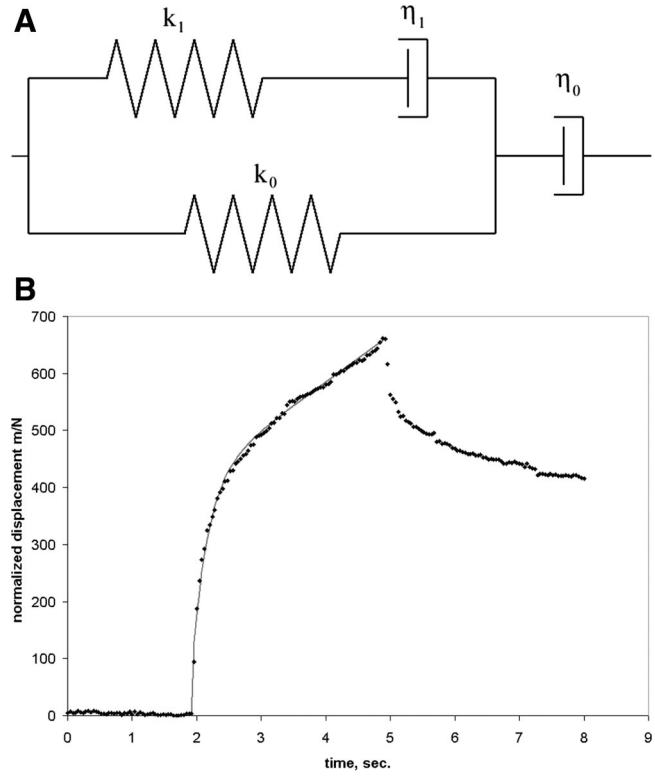

Fig. 2. *A*: the spring-dashpot model consists of a Kelvin body in series with a dashpot to model the motion of magnetic beads attached to cells under a step force. *B*: a typical magnetic bead displacement curve shows the spring's response at 2 s, the creep response from 3 to 5 s, and the subsequent unloading response from 5 to 8 s. The best-fit curve based on the derived parameters is shown as a solid line from 2 to 5 s.

1 A. The displacements of the magnetic beads typically ranged from 0.5 to 3 μm.

Receptor effects on cellular mechanical properties. Using magnetic bead data, the stiffness of the springs and viscosities of the dashpots in the Kelvin receptor-based model were determined (Fig. 2, *A* and *B*). Using 125 beads for the fibronectin endocytosis experiments, 104 beads for the transferrin receptor, and 31 magnetic beads for the dystroglycan receptor on epithelial cells, we found that the median instantaneous stiffnesses were 3.9×10^{-3} N/m for the endocytosed beads, 4.4×10^{-3} N/m for anti-transferrin beads, and 1.6×10^{-3} N/m for the anti-dystroglycan beads (Fig. 3*A*). Each bead represented data from a different cell. The instantaneous stiffness of the dystroglycan receptor was significantly different from both the endocytosed beads ($P < 0.001$) and the transferrin receptor ($P < 0.001$). The viscous friction coefficient of the dystroglycan receptor was significantly different from both the endocytosed beads ($P < 0.05$) and the transferrin receptor ($P < 0.05$; Fig. 3*B*). No significant differences were found regarding the relaxation times of the two receptors and the endocytosed beads (Fig. 3*C*).

With the addition of cytochalasin D to disrupt the actin cytoskeleton, using 89 beads for the fibronectin endocytosis experiments, 47 beads for the transferrin receptor, and 31 magnetic beads for the dystroglycan receptor on epithelial cells, the instantaneous membrane stiffness of the epithelial cells significantly decreased for all conditions ($P < 0.001$ for endocytosed beads and transferrin receptors, $P < 0.05$ for dystroglycan receptors; Fig. 3*A*). Cytochalasin D significantly decreased the viscous friction coefficient for all conditions ($P < 0.001$ for endocytosed beads and transferrin receptors, $P < 0.01$ for dystroglycan receptors; Fig. 3*B*) and increased the relaxation time significantly only for the endocytosed beads ($P < 0.001$; Fig. 3*C*). The addition of cytochalasin D to HEK-293 cells caused disruption of the actin cytoskeleton, as demonstrated by phalloidin staining (Fig. 3, *D* and *E*), but the cells remained spread and attached to the dish, suggesting that at least some of the cytoskeletal components remained intact.

To characterize how well the antibody-coated beads adhered to the cell, antibodies against transferrin receptors and α-dystroglycan were placed into the medium at the same time as the beads to competitively bind the receptors (using 5 μg of antibody in every 1 ml of medium). After incubating for attachment, the sample was perturbed manually to detect loose beads. The detachment rates for initially attached magnetic beads were recorded and compared with the detachment rates for beads on unblocked cells. In both cases, detachment increased when blocking with antibodies was performed. For the transferrin receptor, detachment increased from 17 to 31% when blocked by transferrin antibodies, in contrast to 15% detachment when the cells were blocked by both dystroglycan and anti-β_1 antibodies. The results were similar for dystroglycan, with which detachment increased from 13 to 28% when blocked by anti-dystroglycan antibodies but remained at 11% when blocked by both transferrin and anti-β_1 antibodies. This demonstrates that the bead coatings were fairly specific for targeting the receptors of interest.

The results for smooth muscle cells, in contrast, showed a different mechanical response based on receptors. Using 79 fibronectin beads for endocytosis, 36 transferrin beads, and 60 dystroglycan beads, the median cell stiffness was found to be 4.2×10^{-3} N/m for endocytosed beads, 1.4×10^{-3} N/m using transferrin beads, and 2.6×10^{-3} N/m using dystroglycan beads. A significant difference for stiffness was found only between the endocytosed beads and transferrin receptors (Fig. 4*A*). Significant differences in cellular viscous coefficients were found between the transferrin receptor and both the endocytosed beads ($P < 0.001$) and the dystroglycan receptor ($P < 0.01$) (Fig. 4*B*). No significant differences were found for the relaxation times among the three conditions (Fig. 4*C*).

With the addition of cytochalasin D, cell stiffness significantly decreased only for the endocytosed beads ($P < 0.001$; Fig. 4*A*). However, the viscous coefficient significantly decreased for both endocytosed beads ($P < 0.001$) and dystroglycan receptors ($P < 0.001$; Fig. 4*B*), and the relaxation time significantly increased for all three conditions ($P < 0.001$ for endocytosed beads, $P < 0.05$ for transferrin receptors, and $P < 0.001$ for dystroglycan receptors; Fig. 4*C*).

The presence of cytoskeleton linkage was measured using single-particle tracking. The average displacements of the gold nanoparticles on epithelial cells depended on the type of receptor. As anticipated, the transferrin receptors moved more (median, 1.1 μm; 10 particles) than the dystroglycan receptor (median, 350 nm; 9 particles) and the β_1 integrin (median, 490 nm; 10 particles). The increased motion of the transferrin receptor was significant compared with either the dystroglycan receptor ($P < 0.001$) or the β_1 integrin ($P < 0.05$), whereas the dystroglycan receptors and β_1 integrins were not statistically significantly different (Fig. 5).

DISCUSSION

The use of magnetic micromanipulation has a number of advantages in the analysis of the mechanical properties of living cells, including the ability to control precisely the level and duration of force exerted on the cells, to target specific receptors via selective bead coating, and in some cases, to collect and preserve information on a single-cell basis, which results in obtaining both average and variance information. The main finding of this study is that cell stiffness depends both on the linkage that is being stressed, whether it is the type of surface receptor or internalization, and on the specific cell type that is being probed.

Transferrin receptor-based mechanical stresses result in mechanical properties similar to those of endocytosed beads with epithelial cells. This result is interesting, especially because receptor-tracking experiments using gold nanoparticles have shown that the transferrin receptor is less anchored than the dystroglycan or β_1 integrin receptors. We hypothesize that when a force was applied to the bead, it was distributed to membrane compartments that indirectly transmitted the force to the cytoskeleton. Because compartments are thought to be 0.2–1 μm in diameter (22), a 4.5-μm-diameter bead could easily span several compartments. An estimate for the force on a single transferrin receptor can be obtained by assuming that the receptor density is the same as that reported for HepG2 cells, 5×10^4/cell (36a), and that the cell shape can be approximated as a 15-μm-radius thin disk (see Fig. 1*C*). If the receptors are uniformly distributed on the cell surface, the receptor density in each cell is 3×10^{13} receptors/m^2. We further assume that the bead-cell contact area is circular, with a radius of 2 μm (assuming that the bead is approximately

one-third embedded into the cell as an order-of-magnitude estimate). The contact area is $\sim 1.2 \times 10^{-11}$ m^2, which led us to conclude that the number of receptors associated with each bead was on the order of 400. The typical force applied to each bead is $\sim$1 nN; thus the average force, F, on a single receptor is $\sim$2.5 pN. Because the force-induced displacement, Δx, is on the order of 0.1 μm, the mechanical energy, ΔE, on each receptor can be estimated as $\Delta E = F\Delta x$, or $\sim 2.5 \times 10^{-19}$ J.

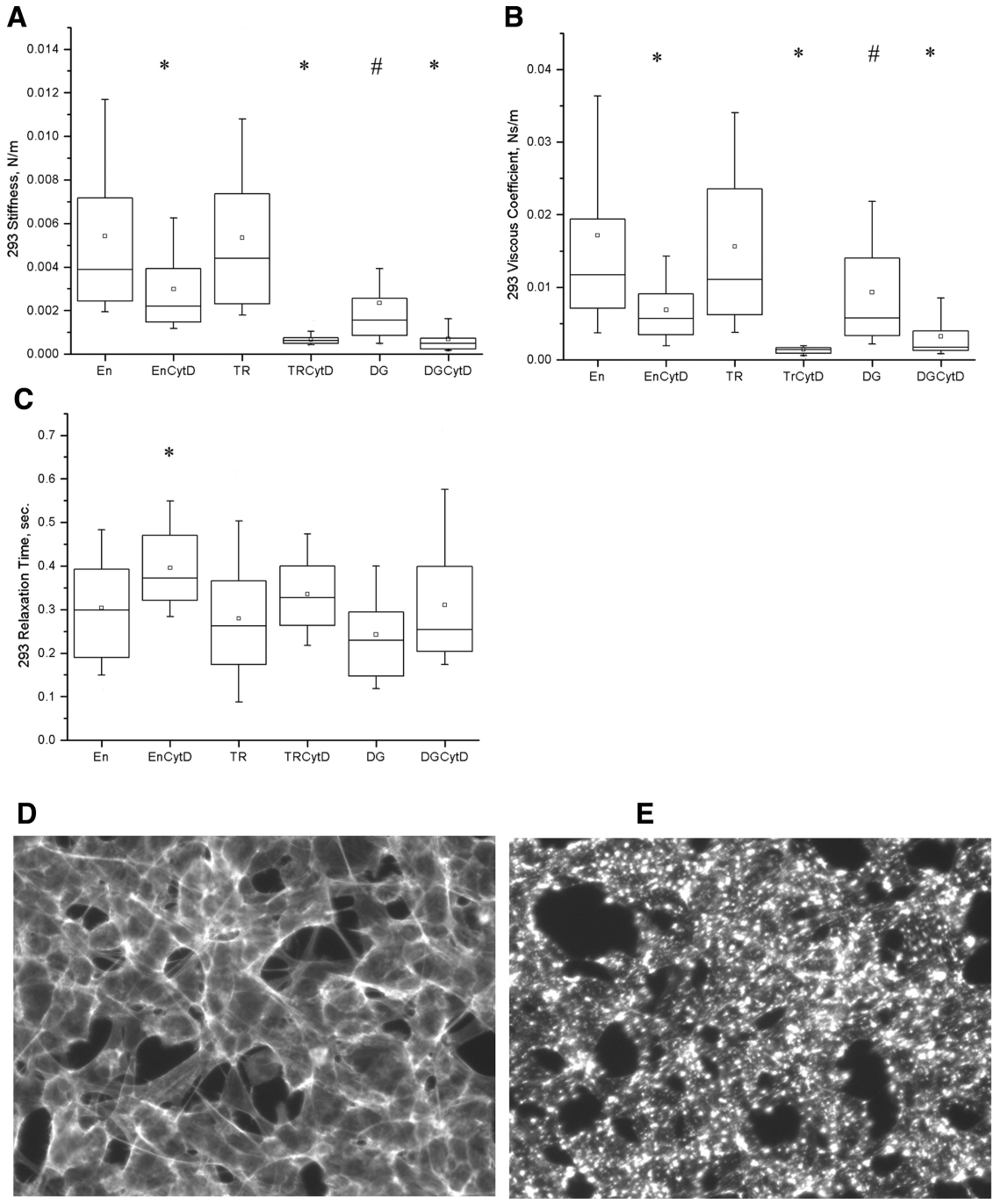

Fig. 3. The stiffness (*A*), viscous friction coefficient (*B*), and relaxation time (*C*) of epithelial cells probed by fibronectin-endocytosed beads (En), transferrin (TR), or dystroglycan (DG) receptors were determined by quantifying the individual component values in the model (Fig. 2*A*) and then combining them (see *Cell model* for formulas). Cells treated with cytochalasin D and probed via the receptors are shown (EnCytD, TRCytD, and DGCytD). Surprisingly, the dystroglycan receptor-based stiffness and viscosity were significantly lower than the transferrin receptor-based stiffness and viscosity. Data are shown as boxplots in which the error bars depict the 5 and 95% percentile values. The main box has three horizontal lines, for 25, 50, and 75% percentile values (the middle bar represents the median), respectively. The small squares represent the means. $*P < 0.05$, statistically significant changes in the parameters with the cytochalasin D-treated cases. $\#P < 0.05$, statistically significant changes among the untreated cases. Thus, in *A*, all conditions were statistically significantly different from the cytochalasin D-treated cases (e.g., En vs. EnCytD), and DG was statistically significantly lower in stiffness than En and TR. *D*: epithelial cells were stained with Oregon green phalloidin to show the presence of f-actin. *E*: upon addition of cytochalasin D, these fibers were disrupted, but the cells remained adherent to the dish. Magnification in *D* and *E*, ×30 (×20 objective with a ×1.5 modifier in the microscope base).

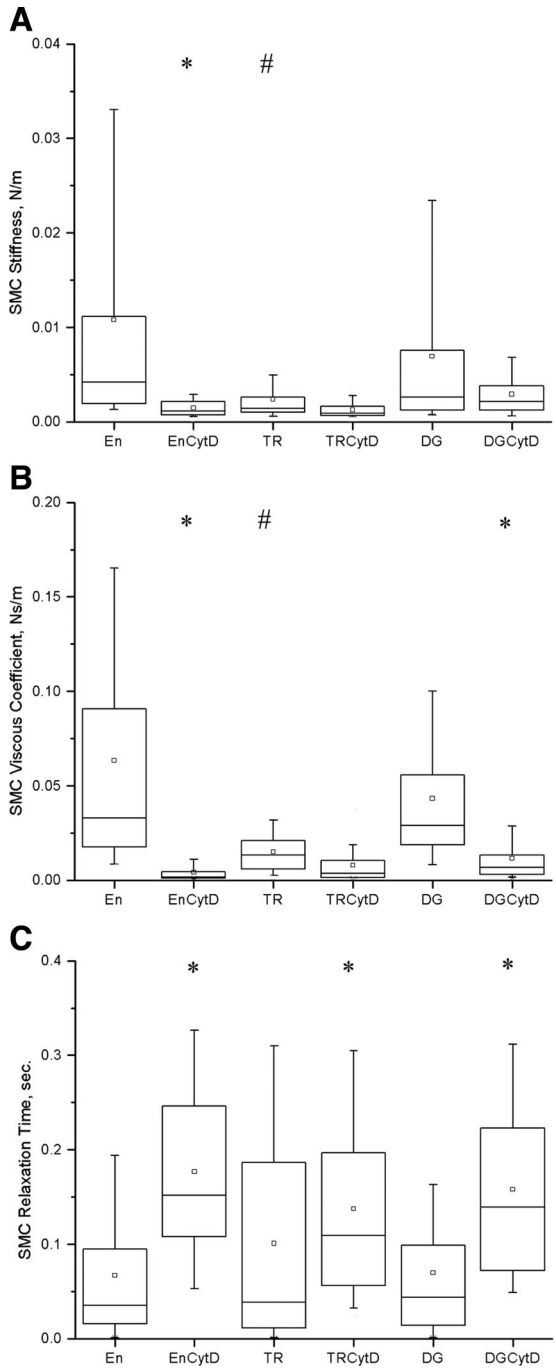

Fig. 4. Spring-dashpot model applied to smooth muscle cells (SMC) revealing different receptor responses to mechanical stresses. The stiffness (*A*), viscous friction coefficient (*B*), and relaxation time (*C*) were approximately the same order of magnitude as those in the epithelial cells, but the relative values for the fibronectin-endocytosed beads (En), transferrin (TR), and dystroglycan (DG) were different. With the addition of cytochalasin, changes similar to those shown in Fig. 3 (e.g., EnCytD) occurred. $*P < 0.05$, statistically significant changes in the parameters in the cytochalasin D-treated cases. $\#P < 0.05$, statistically significant changes among the untreated cases. Note that in *A*, the significant difference (#) was between only fibronectin and transferrin. Data are shown as boxplots as in Fig. 3.

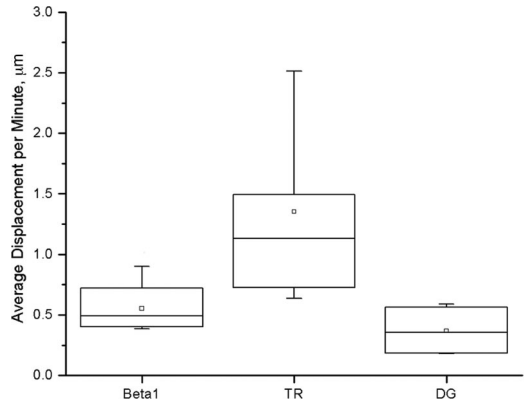

Fig. 5. Average displacement, over 1 min, of nanogold particles attached to the integrin, transferrin, or dystroglycan receptors is shown as a boxplot as in Fig. 3. The transferrin receptors moved significantly farther than either of the other two receptors, supporting the view that transferrin receptors lack direct linkage to the cytoskeleton. Integrin and dystroglycan receptor motion were not statistically significantly different from each other.

The typical energy of a hydrogen bond is on the order of 3.5×10^{-20} J (46). Therefore, the energy exerted on each transferrin receptor is of an equivalent order to 10 hydrogen bonds. It is reasonable to expect that at the molecular level, associations between the transferrin receptor and the surrounding membrane domain structure are not significantly perturbed by the force levels associated with this energy level. Thus the force exerted on each transferrin receptor is likely transmitted directly to the membrane compartments. Because these membrane compartments can also contain proteins that are linked to the cytoskeleton, we hypothesize that the membrane compartments serve as an integrating element that indirectly transmits the sum of the forces on the transferrin receptors to the cellular cytoskeleton. Detailed structural analysis of compartmental protein compositions and associations with the cytoskeleton await further study. Finally, transferrin receptors are associated with endocytotic events (19); thus the similarities between the endocytosed beads and the transferrin-linked beads appear to support a similarity in the cytoskeletal linkage between the two bead types. These explanations are further supported by the observation that when cytochalasin D was added to the cells, the transferrin receptors' stiffness and viscosity decreased more than those of fibronectin (Fig. 3, *A* and *B*). Insufficient cytochalasin D was added to totally disrupt the cell cytoskeleton; thus cell stiffness and viscosity were maintained better for the endocytosed beads' network than for the transferrin receptors' because the transferrin receptor-based stiffness depended on the surface compartmentalization network rather than on being surrounded by a cytoskeletal network as was true for endocytosed beads.

An unexpected finding is that the dystroglycan receptor-based stiffness was lower than that of the transferrin receptor on epithelial cells. Because dystroglycan is linked to the cytoskeleton via dystrophin-utrophin, this lower stiffness is surprising. One possible, intriguing explanation is the introduction of cytoskeletal subnetworks; that is, that the dystroglycan-linked cytoskeleton forms a different network with its own mechanical properties. Assuming the presence of this independent network, the cytochalasin D results are further evidence that this secondary network is affected more severely

by the actions of cytoskeletal disruption. One could conclude that this network consists of a higher percentage of actin than the cytoskeletal network at large.

The smooth muscle cell results, in contrast, show significantly lower cell stiffness for transferrin-linked beads and no differences for dystroglycan-linked beads compared with the endocytosed beads. The apparent increase in stiffness of the dystroglycan receptor relative to the epithelial cells could be explained by differences in the α-dystrogylcan receptor. These receptors, which appear more variably glycosylated in epithelial cells than in smooth muscle cells, may be related to weaker or less prevalent networking when hypoglycosylated (17). At the very least, glycosylation is an indicator of receptor activity and has been hypothesized to be linked to muscular dystrophy (24, 25). That dystroglycan may be in a subnetwork rather than in the global network affecting the endocytosed beads is further supported by results observed after the addition of cytochalasin D; with increased activity of the dystroglycan receptors, the decrease in stiffness of the dystroglycan receptors is much smaller and settles on a stiffness that is higher than that of the endocytosed beads. This indicates that in smooth muscle cells, the dystroglycan network may be more pervasive or may depend less on actin than in epithelial cells because of its apparently higher resistance to cytochalasin D disruption compared with a bead fully surrounded by a partially disrupted cytoskeleton.

The reason for the decreased transferrin receptor stiffness in smooth muscle cells but not in epithelial cells is not as clear. If the compartmentalization network is responsible for the observed transferrin and dystroglycan receptor stiffness in epithelial cells, this network may be absent or configured differently in smooth muscle cells, leading to different behaviors in response to mechanical stresses. Furthermore, the role of transferrin receptors in endocytosis in smooth muscle cells may be different from their role in epithelial cells. Such a result is important, because in many mechanotransduction experiments, non-cytoskeletally linked receptors (e.g., transferrin or the acetylated LDL receptors) are used as a negative control based on the hypothesis that non-cytoskeletally linked receptors do not contribute to mechanically induced signaling (23, 42, 51). Our results indicate that caution is required when interpreting results based solely on known molecular linkages rather than on the actual physical response of the cells. Most bead-based signaling studies used fibroblasts, endothelial cells, and smooth muscle cells, which are vascular cells; however, it is possible that when the cell types are broadened, the signaling results may start to diverge.

The viscous friction coefficient results are consistent with what is expected; the less stiff conditions also tend to have lower viscosities, and the disruption of the actin network by cytochalasin D diminishes the viscosity (although in one case this did not reach statistical significance, this trend is fairly consistent). The relaxation time governs the shape of the response curve in transition to the viscous regime (in Fig. 2*B*, it determines the shape of the curve between 2 and 3 s). Increased relaxation time indicates that it takes longer for the curve to settle on the linear motion determined by the viscous friction coefficient. Interestingly, there are no receptor dependencies for the relaxation time, but the smooth muscle cells show a large increase in this parameter with the addition of cytochalasin D compared with the epithelial cells, indicating that it takes longer to settle to the steady state in the presence of a disrupted actin network.

In interpreting the results of these experiments, some simplifying assumptions are necessary. For example, while the models used in this study to fit the bead displacements are linear, and although it is reasonable to expect living cells not to behave in a strictly linear fashion, there are currently no nonlinear analytical models that can be used with magnetic trapping to describe the simple response of a cell to a fixed applied force. Finite element modeling can help to some extent, and efforts are currently underway to compare magnetic trapping experimental results to finite element models (34). In addition, the model used in this study was analyzed for the loading portion of the magnetic bead displacement only. Improved models that account for the unloading portion may yield other insight into the mechanical response of the cells. Other components of the cytoskeleton, such as the microtubules, were not tested but could potentially have a role in bead response, especially for the endocytosed beads. For example, an alternative possible explanation of the higher stiffness for endocytosed beads compared with transferrin in cytochalasin D-disrupted epithelial cells is that the endocytosed beads experience resistance from other intracellular components such as microtubules and intermediate filaments, even with the actin filaments completely disrupted. That this effect is not seen in the smooth muscle cells, and the possibility that epithelial cells can remain spread with a totally disrupted actin cytoskeleton serves only to underscore the complexity of characterizing general cell mechanical properties.

The number of beads used for each receptor appears roughly correlated with stiffness results (i.e., the results with the fewest number of beads for a given receptor in both the epithelial and smooth muscle experiments were also the receptors with the lowest stiffness). However, it is unlikely that the cellular stiffness results are affected by the number of beads used. Instead, the magnetic beads attached to the lower stiffness receptors also tended to detach at a greater rate. Thus the lower number of postprocessed beads in lower stiffness receptors can be considered a reflection of the lower anchorage of that receptor class.

While each bead was large enough to engage multiple receptors, the use of smaller beads was precluded because of the volume dependency of force generation. Beads small enough to engage single receptors are unlikely to exert sufficient force to generate detectable displacement. Indeed, the relatively high force levels used in this study were necessary to reliably measure the bead displacement in the stiffer cell lines (notably the smooth muscle cells). Because there were likely many receptors engaged for each bead, rolling for the surface receptor-bound beads is not considered to be a major contributor to the mechanical model. As a result, the actual number of receptors engaged for each bead is not likely to make a substantial difference to the fit of the mechanical model. In addition, although it is difficult to relate the extent of rolling of surface beads to that of endocytosed beads, the more important focus of this study was in comparing the two different surface receptors and on the effects of each class on the corresponding cytoskeletally disrupted parameters rather than on a one-to-one comparison of endocytosed bead stiffness to that of transferrin receptors or dystroglycan. Further characterizations of bead attachment and responses await further investigation.

Our experiments have demonstrated that, taken singly, cell stiffness tends to be lower and depends much more on geometric factors (e.g., size and orientation of the cell; data not shown). In this study, only confluent or nearly confluent monolayers were used. While future studies might address issues such as confluency and orientation, we present our data as the results of a first study to characterize the variances in mechanical properties across cell types and receptors using a single technique.

In summary, the experiments and analyses indicate that characterizing the mechanical properties of the cell depend significantly on the receptor probed and the cell type. Stiffness is increased not simply because the receptor is associated with the cytoskeleton but also possibly because of the presence of different intracellular networks and a higher resistance against degradation for the focal adhesion and major cellular structural network.

ACKNOWLEDGMENTS

We thank Nicki Watson of the Whitehead Institute (Cambridge, MA) for assistance with electron microscopy.

GRANTS

This work was supported in part by grants from the National Institutes of Health and the National Aeronautics and Space Administration. R. Barresi was supported by the Muscular Dystrophy Association. K. P. Campbell is an investigator with the Howard Hughes Medical Institute.

REFERENCES

1. **Alenghat FJ, Fabry B, Tsai KY, Goldmann WH, and Ingber DE.** Analysis of cell mechanics in single vinculin-deficient cells using a magnetic tweezer. *Biochem Biophys Res Commun* 277: 93–99, 2000.
2. **Bausch AR, Hellerer U, Essler M, Aepfelbacher M, and Sackmann E.** Rapid stiffening of integrin receptor-actin linkages in endothelial cells stimulated with thrombin: a magnetic bead microrheology study. *Biophys J* 80: 2649–2657, 2001.
3. **Bausch AR, Möller W, and Sackmann E.** Measurement of local viscoelasticity and forces in living cells by magnetic tweezers. *Biophys J* 76: 573–579, 1999.
4. **Bausch AR, Ziemann F, Boulbitch AA, Jacobson K, and Sackmann E.** Local measurements of viscoelastic parameters of adherent cell surfaces by magnetic bead microrheometry. *Biophys J* 75: 2038–2049, 1998.
5. **Block SM, Goldstein LS, and Schnapp BJ.** Bead movement by single kinesin molecules studied with optical tweezers. *Nature* 348: 348–352, 1990.
6. **Brown TD.** Techniques for mechanical stimulation of cells in vitro: a review. *J Biomech* 33: 3–14, 2000.
7. **Butler JP and Kelly SM.** A model for cytoplasmic rheology consistent with magnetic twisting cytometry. *Biorheology* 35: 193–209, 1998.
8. **Caille N, Tardy Y, and Meister JJ.** Assessment of strain field in endothelial cells subjected to uniaxial deformation of their substrate. *Ann Biomed Eng* 26: 409–416, 1998.
9. **Chen CS, Mrksich M, Huang S, Whitesides GM, and Ingber DE.** Geometric control of cell life and death. *Science* 276: 1425–1428, 1997.
10. **Chen J, Fabry B, Schiffrin EL, and Wang N.** Twisting integrin receptors increases endothelin-1 gene expression in endothelial cells. *Am J Physiol Cell Physiol* 280: C1475–C1484, 2001.
11. **Chien S, Li S, and Shyy YJ.** Effects of mechanical forces on signal transduction and gene expression in endothelial cells. *Hypertension* 31: 162–169, 1998.
12. **Choquet D, Felsenfeld DP, and Sheetz MP.** Extracellular matrix rigidity causes strengthening of integrin-cytoskeleton linkages. *Cell* 88: 39–48, 1997.
13. **Cohn RD and Campbell KP.** Molecular basis of muscular dystrophies. *Muscle Nerve* 23: 1456–1471, 2000.
14. **Coral-Vazquez R, Cohn RD, Moore SA, Hill JA, Weiss RM, Davisson RL, Straub V, Barresi R, Bansal D, Hrstka RF, Williamson R, and Campbell KP.** Disruption of the sarcoglycan–sarcospan complex in vascular smooth muscle: a novel mechanism for cardiomyopathy and muscular dystrophy. *Cell* 98: 465–474, 1999.
15. **Dartsch PC, Hammerle H, and Betz E.** Orientation of cultured arterial smooth muscle cells growing on cyclically stretched substrates. *Acta Anat (Basel)* 125: 108–113, 1986.
17. **Durbeej M and Campbell KP.** Biochemical characterization of the epithelial dystroglycan complex. *J Biol Chem* 274: 26609–26616, 1999.
18. **Durbeej M, Henry MD, and Campbell KP.** Dystroglycan in development and disease. *Curr Opin Cell Biol* 10: 594–601, 1998.
19. **Enns CA, Rutledge EA, and Williams AM.** The transferrin receptor. *Biomembranes* 4: 255–287, 1996.
20. **Fabry B, Maksym GN; Hubmayr RD; Butler JP; and Fredberg JJ.** Implications of heterogeneous bead behavior on cell mechanical properties measured with magnetic twisting cytometry. *J Magnetism Magn Mater* 194: 120–125, 1999.
21. **Fabry B, Maksym GN, Shore SA, Moore PE, Panettieri RA Jr, Butler JP, and Fredberg JJ.** Time course and heterogeneity of contractile responses in cultured human airway smooth muscle cells. *J Appl Physiol* 91: 986–994, 2001.
22. **Fujiwara T, Ritchie K, Murakoshi H, Jacobson K, and Kusumi A.** Phospholipids undergo hop diffusion in compartmentalized cell membrane. *J Cell Biol* 157: 1071–1081, 2002.
23. **Goldschmidt ME, McLeod KJ, and Taylor WR.** Integrin-mediated mechanotransduction in vascular smooth muscle cells: frequency and force response characteristics. *Circ Res* 88: 674–680, 2001.
24. **Grewal PK and Hewitt JE.** Glycosylation defects: a new mechanism for muscular dystrophy? *Hum Mol Genet* 12: R259–R264, 2003.
25. **Grewal PK, Holzfeind PJ, Bittner RE, and Hewitt JE.** Mutant glycosyltransferase and altered glycosylation of α-dystroglycan in the myodystrophy mouse. *Nat Genet* 28: 151–154, 2001.
26. **Heidemann SR, Kaech S, Buxbaum RE, and Matus A.** Direct observations of the mechanical behaviors of the cytoskeleton in living fibroblasts. *J Cell Biol* 145: 109–122, 1999.
27. **Henry MD and Campbell KP.** Dystroglycan: an extracellular matrix receptor linked to the cytoskeleton. *Curr Opin Cell Biol* 8: 625–631, 1996.
28. **Hishikawa K and Lüscher TF.** Pulsatile stretch stimulates superoxide production in human aortic endothelial cells. *Circulation* 96: 3610–3616, 1997.
29. **Holt KH and Campbell KP.** Assembly of the sarcoglycan complex: insights for muscular dystrophy. *J Biol Chem* 273: 34667–34670, 1998.
30. **Ilsley JL, Sudol M, and Winder SJ.** The WW domain: linking cell signalling to the membrane cytoskeleton. *Cell Signal* 14: 183–189, 2002.
31. **Ingber DE.** Cellular tensegrity: defining new rules of biological design that govern the cytoskeleton. *J Cell Sci* 104: 613–627, 1993.
32. **Ingber DE.** Tensegrity: the architectural basis of cellular mechanotransduction. *Annu Rev Physiol* 59: 575–599, 1997.
33. **Ingber DE, Prusty D, Sun Z, Betensky H, and Wang N.** Cell shape, cytoskeletal mechanics, and cell cycle control in angiogenesis. *J Biomech* 28: 1471–1484, 1995.
34. **Karcher H, Lammerding J, Huang H, Lee RT, Kamm RD, and Kaazempur-Mofrad MR.** A three-dimensional viscoelastic model for cell deformation with experimental verification. *Biophys J* 85: 3336–3349, 2003.
35. **Kuo SC and Sheetz MP.** Force of single kinesin molecules measured with optical tweezers. *Science* 260: 232–234, 1993.
36. **Lammerding J, Kazarov AR, Huang H, Lee RT, and Hemler ME.** Tetraspanin CD151 regulates α6β1 integrin adhesion strengthening. *Proc Natl Acad Sci USA* 100: 7616–7621, 2003.

36a. **Lauffenburger DA and Linderman JJ.** *Receptors: Models for Binding, Trafficking, and Signaling.* New York: Oxford University, 1993.

37. **Lee AA, Delhaas T, McCulloch AD, and Villarreal FJ.** Differential responses of adult cardiac fibroblasts to in vitro biaxial strain patterns. *J Mol Cell Cardiol* 31: 1833–1843, 1999.
38. **Lim LE and Campbell KP.** The sarcoglycan complex in limb-girdle muscular dystrophy. *Curr Opin Neurol* 11: 443–452, 1998.
39. **Lyall F, Deehan MR, Greer IA, Boswell F, Brown WC, and McInnes GT.** Mechanical stretch increases proto-oncogene expression and phosphoinositide turnover in vascular smooth muscle cells. *J Hypertens* 12: 1139–1145, 1994.
40. **Matsumura K and Campbell KP.** Deficiency of dystrophin-associated proteins: a common mechanism leading to muscle cell necrosis in severe childhood muscular dystrophies. *Neuromuscul Disord* 3: 109–118, 1993.

41. **McNamee HP, Liley HG, and Ingber DE.** Integrin-dependent control of inositol lipid synthesis in vascular endothelial cells and smooth muscle cells. *Exp Cell Res* 224: 116–122, 1996.
42. **Pommerenke H, Schreiber E, Durr F, Nebe B, Hahnel C, Möller W, and Rychly J.** Stimulation of integrin receptors using a magnetic drag force device induces an intracellular free calcium response. *Eur J Cell Biol* 70: 157–164, 1996.
43. **Potard US, Butler JP, and Wang N.** Cytoskeletal mechanics in confluent epithelial cells probed through integrins and E-cadherins. *Am J Physiol Cell Physiol* 272: C1654–C1663, 1997.
44. **Pourati J, Maniotis A, Spiegel D, Schaffer JL, Butler JP, Fredberg JJ, Ingber DE, Stamenovic D, and Wang N.** Is cytoskeletal tension a major determinant of cell deformability in adherent endothelial cells? *Am J Physiol Cell Physiol* 274: C1283–C1289, 1998.
45. **Stamenovic D, Fredberg JJ, Wang N, Butler JP, and Ingber DE.** A microstructural approach to cytoskeletal mechanics based on tensegrity. *J Theor Biol* 181: 125–136, 1996.
46. **Stryer L.** *Biochemistry* (4th ed.). New York: Freeman, 1995.
47. **Thoumine O and Ott A.** Time scale dependent viscoelastic and contractile regimes in fibroblasts probed by microplate manipulation. *J Cell Sci* 110: 2109–2116, 1997.
48. **Thoumine O, Ott A, Cardoso O, and Meister JJ.** Microplates: a new tool for manipulation and mechanical perturbation of individual cells. *J Biochem Biophys Methods* 39: 47–62, 1999.
49. **Wagner CT, Durante W, Christodoulides N, Hellums JD, and Schafer AI.** Hemodynamic forces induce the expression of heme oxygenase in cultured vascular smooth muscle cells. *J Clin Invest* 100: 589–596, 1997.
50. **Wang H, Ip W, Boissy R, and Grood ES.** Cell orientation response to cyclically deformed substrates: experimental validation of a cell model. *J Biomech* 28: 1543–1552, 1995.
51. **Wang N, Butler JP, and Ingber DE.** Mechanotransduction across the cell surface and through the cytoskeleton. *Science* 260: 1124–1127, 1993.
52. **Wang N and Ingber DE.** Control of cytoskeletal mechanics by extracellular matrix, cell shape, and mechanical tension. *Biophys J* 66: 2181–2189, 1994.
53. **Wang N and Ingber DE.** Probing transmembrane mechanical coupling and cytomechanics using magnetic twisting cytometry. *Biochem Cell Biol* 73: 327–335, 1995.
54. **Wang N, Naruse K, Stamenović D, Fredberg JJ, Mijailovich SM, Tolić-Norrelykke IM, Polte T, Mannix R, and Ingber DE.** Mechanical behavior in living cells consistent with the tensegrity model. *Proc Natl Acad Sci USA* 98: 7765–7770, 2001.